DISCLAIMER

This report was prepared as an account of work sponsored by an agency of the United States Government. Neither the United States Government nor any agency thereof, nor any of their employees, makes any warranty, express or implied, or assumes any legal liability or responsibility for the accuracy, completeness, or usefulness of any information, apparatus, product, or process disclosed, or represents that its use would not infringe privately owned rights. Reference herein to any specific commercial product, process, or service by trade name, trademark, manufacturer, or otherwise does not necessarily constitute or imply its endorsement, recommendation, or favoring by the United States Government or any agency thereof. The views and opinions of authors expressed herein do not necessarily state or reflect those of the United States Government or any agency thereof. Reference herein to any social initiative (including but not limited to Diversity, Equity, and Inclusion (DEI); Community Benefits Plans (CBP); Justice 40; etc.) is made by the Author independent of any current requirement by the United States Government and does not constitute or imply endorsement, recommendation, or support by the United States Government or any agency thereof.

ORNL/TM-2024/3427
CRADA/NFE-20-08381

Design of Novel Hot Gas Path Component for Gas Turbine Engines Enabled by Materials and Additive Manufacturing Process Development

Julio Rojas
Patxi Fernandez
Michael Kirka
Frank Brinkley
Chris Ledford
Daniel Ryan
Sudhakar Bollapragada

June 2024

OAK RIDGE National Laboratory

ORNL IS MANAGED BY UT-BATTELLE LLC FOR THE US DEPARTMENT OF ENERGY

ORNL/TM-2024/3427

Manufacturing Science Division

DESIGN OF NOVEL HOT GAS COMPONENTS FOR GAS TURBINE ENGINES ENABLED BY MATERIALS AND ADDITIVE MANUFACTURING PROCESS DEVELOPMENT

Julio Ortega Rojas
Patxi Fernandez-Zelaia
Michael Kirka
Frank Brinkley
Chris Ledford
Daniel Ryan
Sudhakar Bollapragada

June 2024

Prepared by
OAK RIDGE NATIONAL LABORATORY
Oak Ridge, TN 37831
managed by
UT-BATTELLE LLC
for the
US DEPARTMENT OF ENERGY
under contract DE-AC05-00OR22725

CONTENTS

ABSTRACT

Additive Manufacturing (AM), also known as 3D printing, has emerged as a manufacturing method that enables new design freedom for gas turbine engine manufacturers. However, the material selection for AM processable high-temperature superalloys is currently limited. Additionally, the heat transfer performance of AM enabled micro-cooling architectures is not yet well understood. Accordingly, in support of advanced manufacturing and engine performance development, Oak Ridge National Laboratory (ORNL) and Solar Turbines (Solar) conducted a multidisciplinary project to generate both AM superalloy material properties data and micro-channel performance data for two AM superalloys. The data supported the design and analysis of an internally cooled turbine hot section AM tip shoe component. This data was used to analytically predict the reduction in operating temperature of a gas turbine tip shoe. The work concluded that the cooling flow required to cool the tip shoe can be tuned to suit the efficiency improvements desired in an industrial gas turbine.

1. Background

This CRADA project was the result of a project award under FOA-DOE-0001980. The overarching FOA project team consisted of researchers from Carpenter Technology Corporation (CTC), Solar Turbines Incorporated (Solar), Pennsylvania State University (PSU), University of California-Santa Barbara (UCSB), and Oak Ridge National Laboratory (ORNL). Evaluations were conducted on two high-γ' superalloys that were designed by CTC and the UCSB. One alloy named GammaPrint-700 (GP-700) is a cobalt-base superalloy. The other alloy named GammaPrint-1100 (GP-1100) is a nickel-base (Ni-base) superalloy. PSU provided expertise and experimental testing of the thermal performance of AM micro-cooling architectures. ORNL provided expertise with the AM superalloy materials characterization and AM processing science. Solar provided turbine component design expertise. The focus of this CRADA report is to document the efforts between ORNL and Solar Turbines towards the design of an AM superalloy cooled tip shoe.

The project goal was to use an AM processable high-temperature superalloy and design for Additive Manufacturing (DfAM) techniques to design an efficient turbine component (i.e. a turbine tip shoe) with enhanced cooling features that can only be fabricated through additive manufacturing (AM). The efficiencies of existing combined heat and power (CHP) engines are capped by both component design and materials limitations. However, AM of a tip shoe component from a γ'strengthened superalloy offers the design flexibility to increase the efficiency and power of an industrial gas turbine.

This project brought about advancements in the DfAM tip shoe design space and in the area of high temperature superalloys processable through laser powder bed fusion (LPBF) AM. State of art computation design tools were utilized to optimize unique cooling features into a tip shoe component design. A two-prong materials development approach was taken to support development of the AM tip shoe geometry. The first approach centered on investigating the processability and the appropriate process science for the industry standard high-γ' nickel-base (Ni-base) superalloy Mar-M247. This superalloy is typically cast and considered non-weldable by traditional welding standards. In the course of this work, the alloy was not deemed feasible for process scale-up due to significant cracking issues during printing. The second approach focused

on the development and evaluation of a novel cobalt-base superalloy, GammaPrint™-700 (GP-700 and a Ni-base superalloy, GammaPrint™-1100 (GP-1100) designed to mitigate the significant AM processing issues with Mar-M247. The processability of these two alloys were investigated through electron beam melting (EBM), binder-jet AM (BJAM), and laser powder bed fusion (LPBF) as a risk mitigation for manufacturability. To be considered a candidate material for down-selection to proceed to full-scale AM tip shoe engine testing trials, the high temperature creep rupture strength was required to achieve at a minimum, a Larsen Miller Parameter (LMP) increase of 10.9% over the baseline material LPBF AM Hastelloy X.

2. TECHNICAL RESULTS

2.1 PRINTING

Initially this project focused on evaluation of three alloys (GP-700, GP-1100, and Mar-M247) across three AM technologies (LPBF, EBM, and BJAM). Mar-M247 was found to be too crack prone across all three printing technologies. Processing of both GP-700 and GP-1100 via EBM-AM was successful, however, the need for fine spatial resolution in the tip shoe components favored the use of LPBF. Binder-jet AM was found to require significant binder development to allow for successful sintering of the alloys. Hence, this report focuses on the LPBF processing of both the Ni and Co based superalloys, GP-700 and GP-1100 respectively.

Builds consisting of design of experiments (DoE) for both materials (GP-700 and GP-1100) were executed at ORNL utilizing the EOS M290 LPBF machine platform. Several DoEs were performed to assess the calibration of the machines used for printing and the repeatability of the process parameters for each material *(*Figure 1). These DoE's were performed to investigate both bulk material density, overhang printability, microstructure, as well as surface roughness characteristics.

2.1.1 GP-700 Printing

A total of 10 prints were completed using GP-700. Multiple parameter studies were performed using a central composite design (CCD) to investigate the design space for GP-700. Based on density and microstructural data, a parameter set that optimized print speed was observed to be significantly faster than that of the process set initially identified by CTC during feasibility trials early in the program. While a high throughput process window was identified, with these parameters a significant difference in texture was observed in the as-printed material (Figure 2). As a result, both the CTC and fast process parameters were utilized to print mechanical test bar samples. The material from the CTC process parameters is referred to as "coarse" microstructure and the high throughput material as "fine" microstructure GP-700 based on the observed microstructure attributes. The high throughput process parameter window had the potential to yield a 50% increased throughput, which on the actual tip shoe components this would reduce a print from one week to three days.

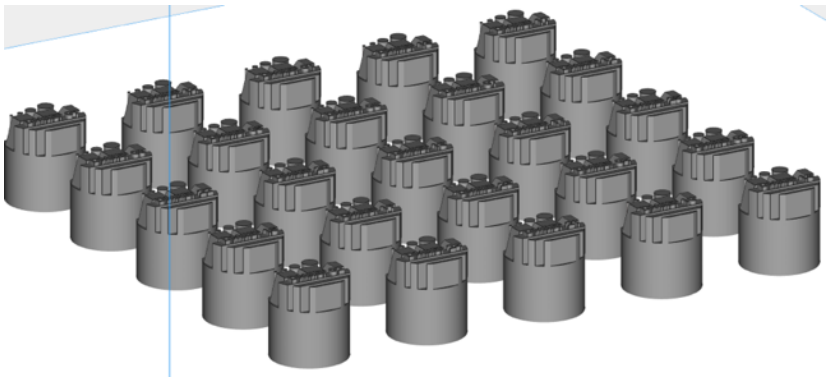

Figure 1 Representative example of the arrays of the geometry utilized for the process parameter development.

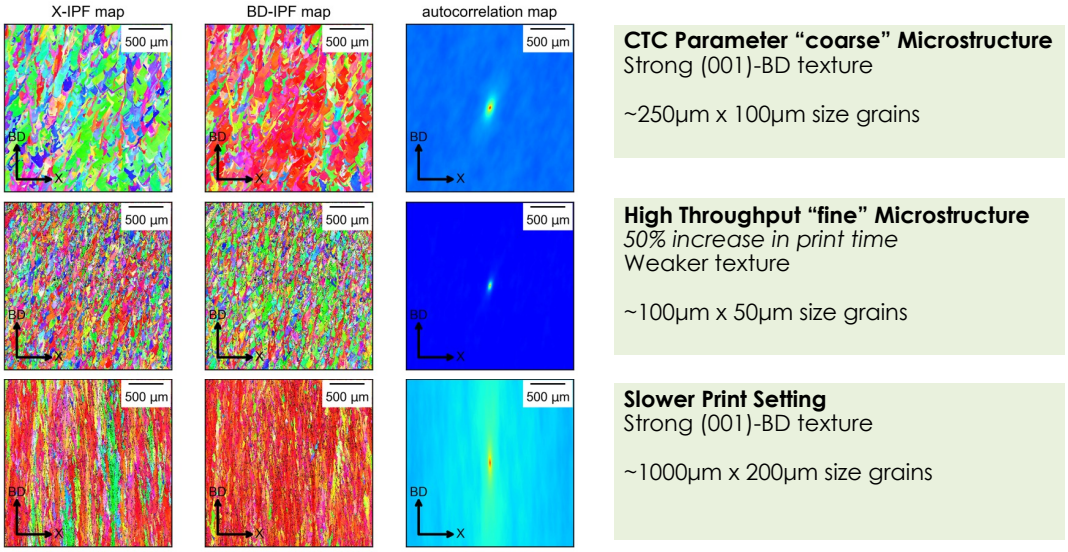

Figure 2: LPBF printed GP-700 Co-superalloy material. (top) CTC printed material (middle) ORNL 'fast' setting (bottom) ORNL 'slow' settings.

2.1.2 GP-1100 Printing

A total of 25 prints were completed using GP-1100 material in an EOS M290 LPBF system utilizing the geometry previously shown in Figure 1 of 2.1.1. Multiple CCD parameter studies were performed to analyze the impact of process parameters on microstructure, mechanical properties, and surface finish of applicable geometries (overhanging pin fins). Based on initial microstructural comparison, the optimal parameters for density and speed remained the parameters developed at CTC early in the initial development efforts of the project and were utilized for all subsequent mechanical test bars prints and the component prints discussed in 2.4.

2.2 HEAT-TREATMENT & MICROSTRUCTURE CHARACTERIZATION

Heat-treatment studies were conducted on GP-700 to understand the recrystallization behavior of the as-printed material, with a desire to retain the columnar grain structure while maximizing the fraction of precipitates that are solutioned, and also to look at maximizing the ductility of the material in the historical superalloy ductility dip regime of 700-800 ºC. Lower temperature stress relief (1000˚C, 1050˚C and 1100˚C) treatments followed by subsolvus (1190˚C) or supersolvus (1215˚C or 1250˚C) treatments were first investigated, Figure 3. The stress relief treatments did not suppress the tendency for recrystallization during supersolvus treatment, even for short times just above the solvus. Subsolvus aging resulted in a fine-scale bimodal precipitate structure that is related to the original cellular structure in the as-printed material.

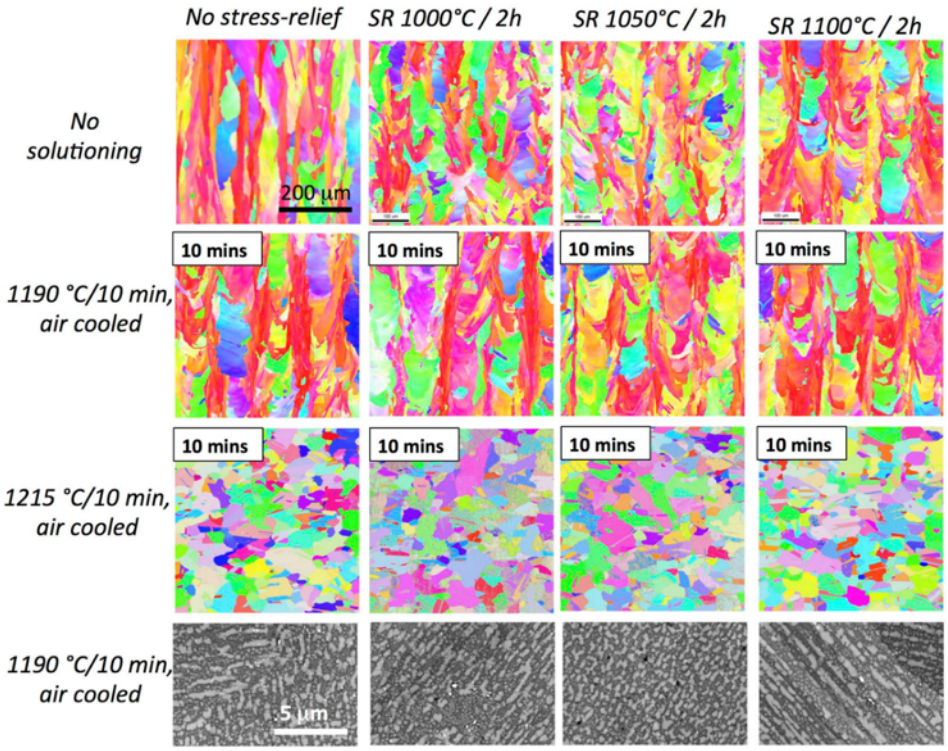

Figure 3: Results of heat treatments of as-printed Co-based superalloy. Top 3 rows are EBSD analyses showing columnar structure retained in subsolvus heat treatments and complete recrystallization in supersolvus. Bottom row shows morphology of strengthening precipitates for each combination of stress relief and heat treatment.

Similar to GP-700, the heat-treatment study for GP-1100 focused on retention of the as-printed columnar structure and examining the recrystallization temperature of the material. Based on differential scanning calorimetry (DSC) the critical temperature for GP-1100 were determined to be: 1162 °C (γ' solvus onset), 1191 °C (γ' solvus completion), 1297 °C (solidus temperature) and 1371 °C (liquidus temperature). Through the heat-treatment study (Figure 4), the grain structure of GP-1100 was found to remain stable below the solvus temperature when solutioned at both 1177 and 1190 ºC. Above the solvus temperature when solutioned at 1215 ºC, the grain structure underwent recrystallization (Figure 4c) with moderate grain growth during the thermal exposure.

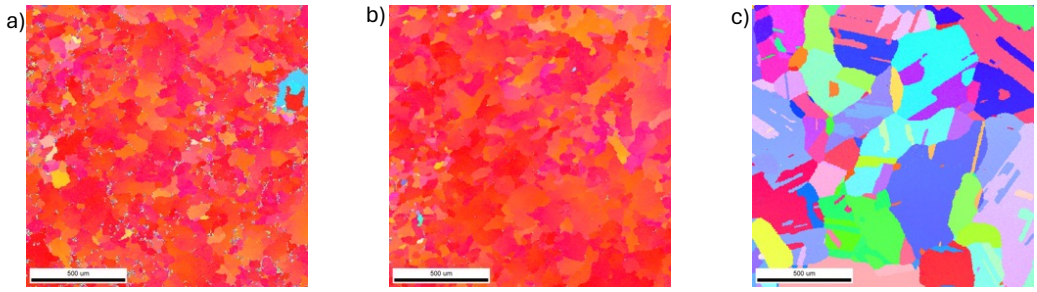

Figure 4: EBSD micrographs of GP-1100 after solution treatments (ST) and air cooling (AC) subsolvous and supersolvous temperatures a) 1177 °C ST and 4hrs AC b) 1190 °C ST and 1hr AC c) ST 1215 °C and 1hr AC

2.3 MECHANICAL TESTING

The mechanical integrity of the LPBF fabricated GP-700 and GP-1100 were evaluated via an experimental plan considering high temperature quasi-static tensile, fatigue, and creep tests to which the performance of the alloys was base-lined against LPBF Hastelloy X.

Thermal-Physical Properties

The thermal conductivity and coefficient of thermal expansion (CTE) of the two candidate AM superalloys were measured at an independent commercial laboratory per ASTM standards from room temperature to 1093°C (2,000°F). Thermal conductivity was calculated from the product of Thermal Diffusivity (ASMT E1461), density (calculated from sample mass & geometry), and specific heat (ASTM E1269). The coefficient of thermal expansion was measured with a dual push-rod dilatometer per ASTM test procedure E228. Sample testing was performed in orientations that were parallel and perpendicular to the build direction to assess for anisotropic behaviour.

The cobalt superalloy GP-700 displayed a slightly higher thermal conductivity values when compared to the nickel superalloy GammaPrint 1100. Both alloys generally showed isotropic thermal conductivity behavior (Table 1, Figure 5).

For Coefficient of Thermal Expansion, the cobalt superalloy GP-700 displayed higher coefficient of thermal expansion values when compared to the nickel superalloy GP-1100. Both alloys generally showed isotropic CTE (Table 2, Figure 6).

Table 1. Thermal Conductivity (btu/hr-ft-°F) experimental test results for AM superalloys GP-700 and GP-1100

Temperature (F)	GammaPrint-700 Horizontal	GammaPrint-700 Vertical	GammaPrint-1100 Horizontal	GammaPrint-1100 Vertical
70.0	5.12	4.99	4.55	4.71
125.0	5.45	5.29	4.79	4.96
200.0	5.89	5.70	5.18	5.37
400.0	7.02	6.77	6.16	6.39
600.0	8.00	7.68	7.10	7.36
800.0	8.88	8.60	8.01	8.27
1000.0	9.75	9.42	8.97	9.06
1200.0	10.81	10.58	9.75	10.07
1400.0	11.84	11.56	10.56	10.96
1600.0	11.49	11.22	10.67	11.07
1800.0	12.23	11.96	11.26	11.56
2000.0	13.03	12.76	11.71	11.95

Table 2. Coefficient of Thermal Expansion (micro in/in °F) experimental test results for AM superalloys GP-700 and GP-1100

Temperature (F)	GammaPrint-700 Horizontal	GammaPrint-700 Vertical	GammaPrint-1100 Horizontal	GammaPrint-1100 Vertical
200.0	7.03	7.03	6.48	6.53
300.0	7.18	7.16	6.59	6.62
400.0	7.29	7.26	6.68	6.71
500.0	7.38	7.35	6.74	6.76
600.0	7.46	7.44	6.81	6.82
700.0	7.55	7.53	6.89	6.88
800.0	7.64	7.62	6.96	6.95
900.0	7.74	7.71	7.04	7.02
1000.0	7.83	7.81	7.13	7.09
1100.0	7.93	7.9	7.25	7.21
1200.0	8.12	8.09	7.4	7.36
1300.0	8.35	8.3	7.53	7.48
1400.0	8.57	8.52	7.63	7.58
1500.0	8.8	8.74	7.79	7.72
1600.0	9.03	8.96	7.95	7.89
1700.0	9.26	9.18	8.17	8.1
1800.0	9.5	9.42	8.43	8.38
1900.0	9.76	9.71	8.74	8.69
2000.0	10.04	10.06	9.1	9.05

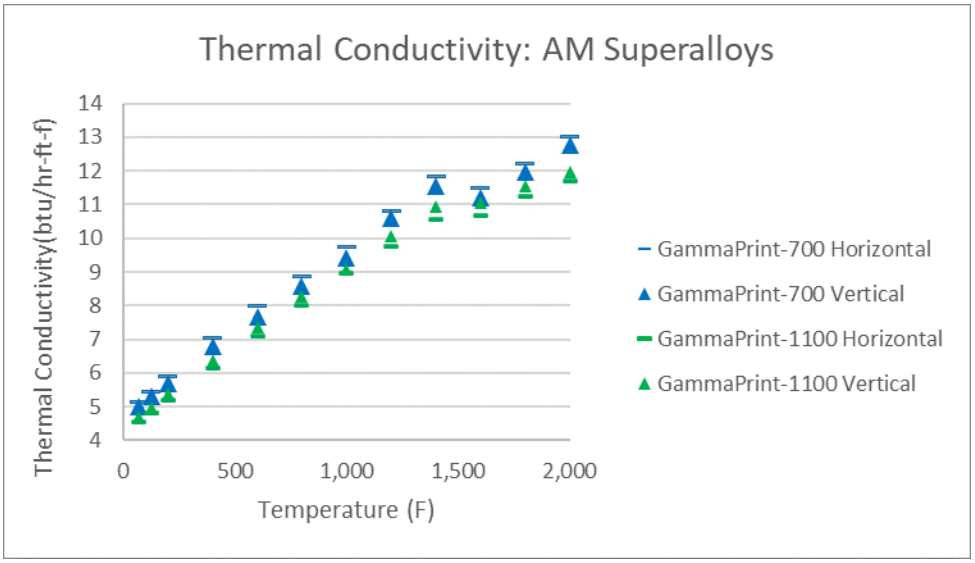

Figure 5. Graph of Thermal Conductivity experimental test results of AM superalloys GP-700 and GP-1100

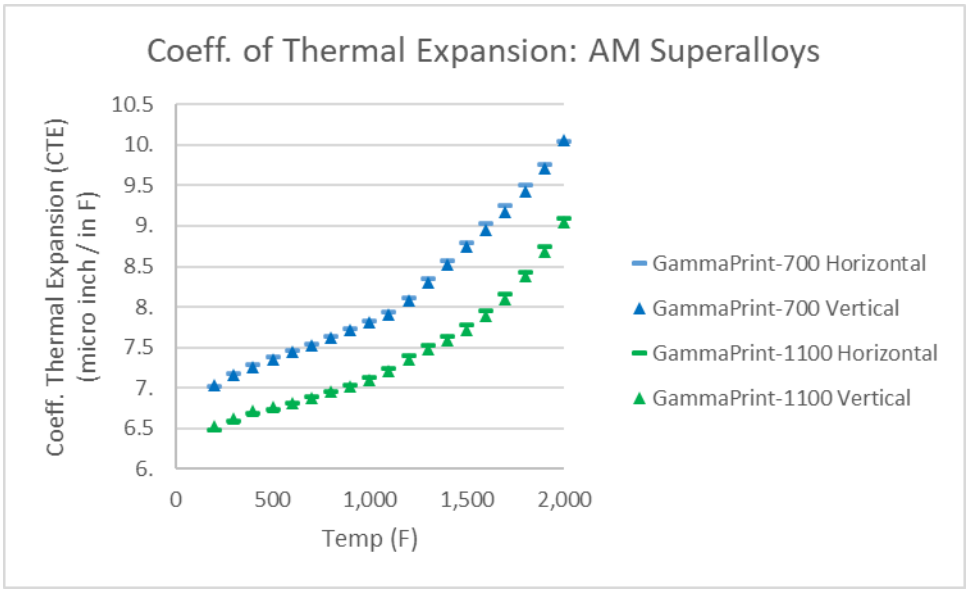

Figure 6. Graph of Coefficient of Thermal Expansion experimental test results of AM superalloys GP-700 and GP-1100

Tensile Properties

The summary of the 0.2% yield stress measured through quasi-static tensile tests for GP-700 and GP-1100 across various temperatures can be seen in Figure 7. Both alloys exhibit the classic ductility dip regime, driven by precipitate-scale deformation mechanisms, in the 750 ºC+ regime. At 800 ºC+ GP-700 and GP-1100 perform similarly to one another.

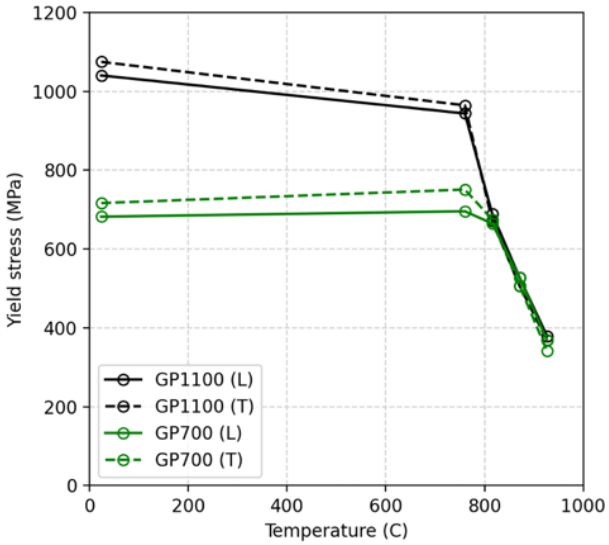

Figure 7. Yield stress of GP-700 and GP-1100 parallel (L) to the build direction and transverse (T) to the build direction.

Creep Properties

Creep testing results, summarized via the Larson-Miller parameter, are shown in Figure 8. Reference curves are included for AM Hastelloy X [1], a 10% curve used as a target in this project, and a 22% stretch goal corresponding to MarM247 behavior [2]. Transverse and longitudinal tests are included. Several points are still 'incomplete' indicating that they may fall even further towards the right of the plot. In summary, the minimum targeted properties were achieved and at higher stress values the 10% reference curve is exceeded for both GP-700 and GP-1100 alloys.

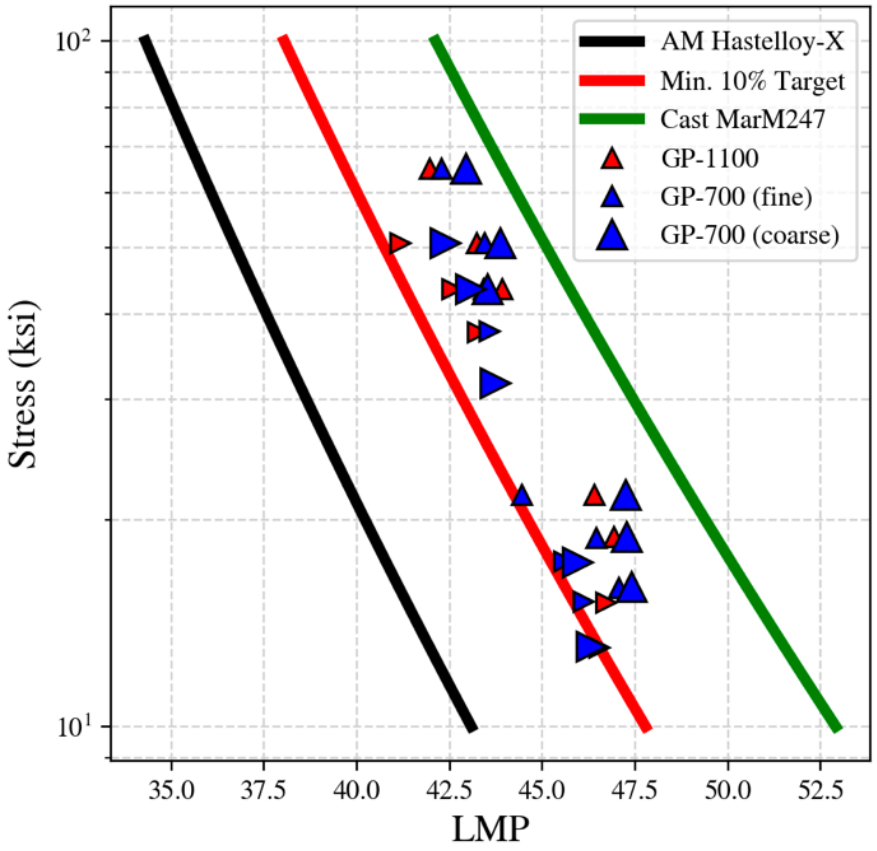

Figure 8. Creep rupture of GP-700, GP-1100, and reference data/curves [1,2]. Two microstructures are included for GP-700. Horizontal markers indicate loading transverse to the BD, vertical markers indicate loading in the BD.

Fatigue Properties

Fatigue results are shown in Figure 9. It should be noted that two sets of GP-700 were fabricated using differing LPBF parameters to produce the two distinctly different microstructures discussed previously. For the purpose of the mechanical testing these are referred to as 'fine' and 'coarse' in relation to the grain sizes. As a reference Hastelloy X fatigue points at 760 °C, the fatigue testing temperature, are also included [3]. The GP-1100 data, in both longitudinal and transverse directions, exceeds the Hastelloy-X behavior. Longitudinally tested coarse grain GP-700 demonstrates exceptionally good fatigue performance, however, the transversely loaded material exhibits a significant debit.

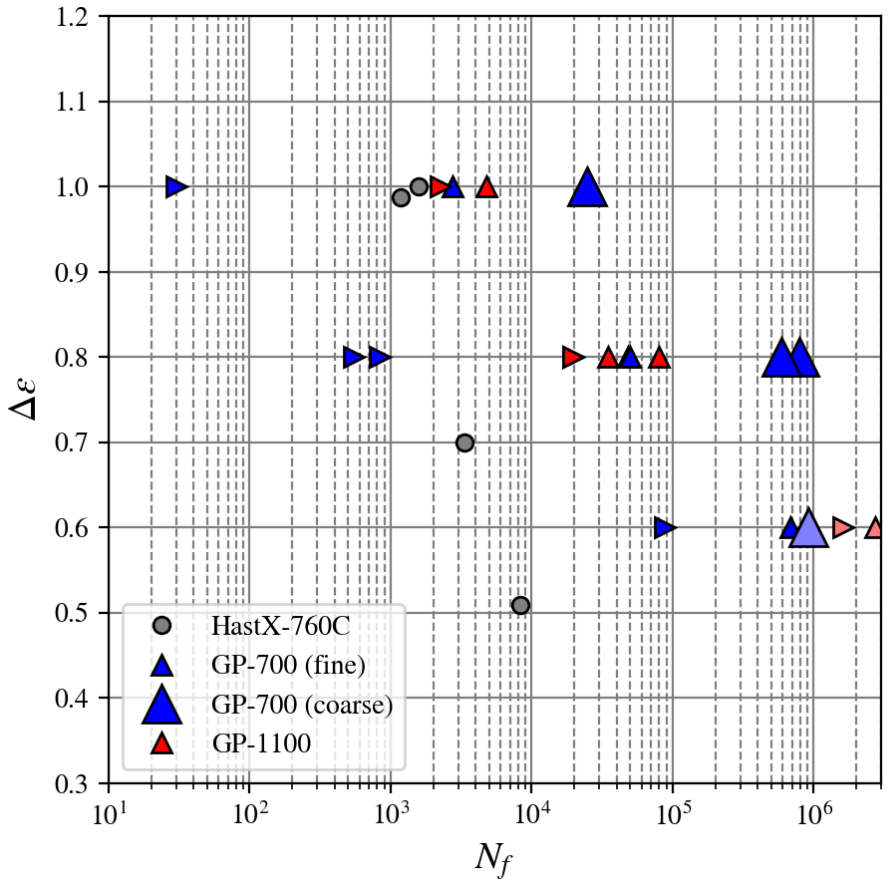

Figure 9. Fatigue results for GP-700 and GP-1100. Vertical triangles denote material aligned with the print direction. Horizontal triangles reference material built perpendicular to the build direction. Reference Hastelloy X included [3].

2.4 AM TIP SHOE COMPONENT DESIGN

2.4.1 AM Micro-Channel Performance

On behalf of Solar Turbines, The Penn State University (PSU) Steady Thermal Aero Research Turbine (START) laboratory incorporated three micro-channel shapes into a flat coupon geometry suitable for laboratory thermal performance testing (Figure 10). Three different AM enabled micro-channel cooling architectures were tested and considered for incorporation into the AM cooled tip shoe component geometry: (1) wavy channels, (2) Pin Fins, and (3) Lattice Structures. A number of coupons were designed with systematic variations in the micro-channel feature geometries. The AM micro-channel coupons were printed in AM Hastelloy® X baseline material by the Penn State CIMP-3D laboratory (Figure 11).

The heat transfer characteristics (Nusselt number, Nu) and friction factor (f) of the AM microchannel coupons were measured on the START lab test rig (Figure 12). Both the Nusselt number and the friction factor of the AM micro-channels showed significant increases when compared to conventionally manufactured smooth channel performance (Figure 13, Figure 14). For more detailed results see reference papers in Appendix A.

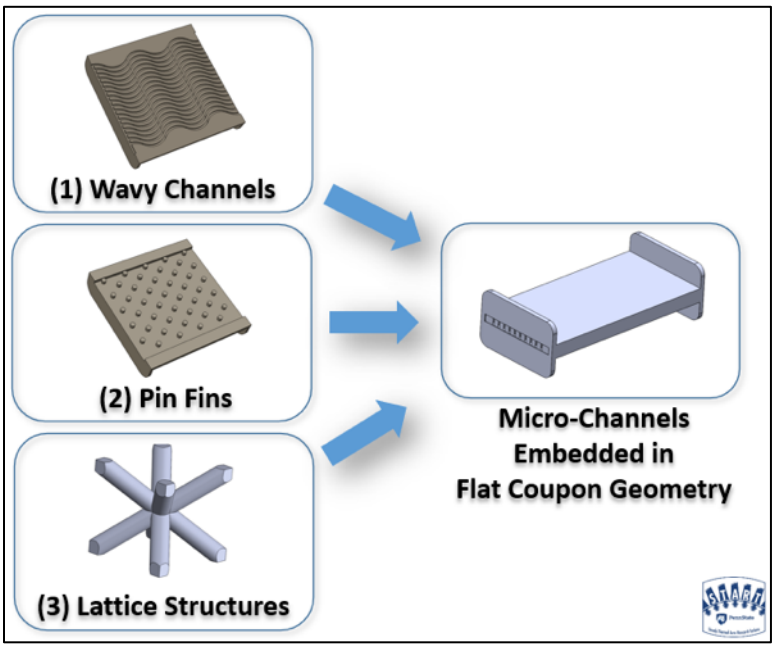

Figure 10. Images of Penn State University START Lab heat transfer rig coupons showing the three AM enabled micro-channel cooling architectures considered for incorporation into the AM tip shoe component design: Wavey Channels (left), Pin Fin Arrays (Center), and Lattice Structure (Right)

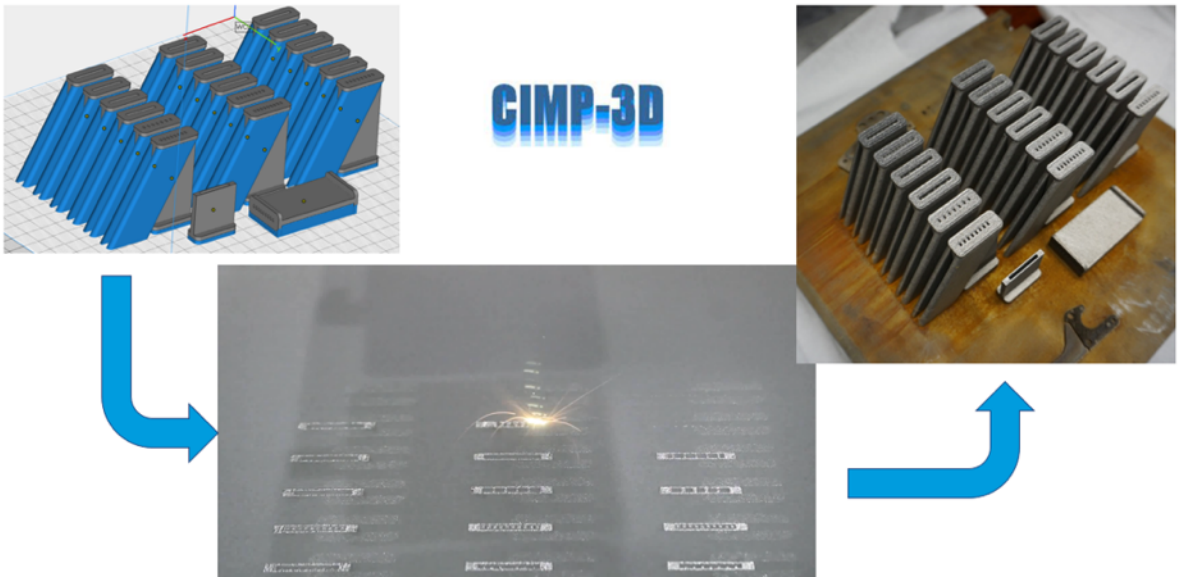

Figure 11 Images showing the Laser Powder Bed Fusion (LPBF) additive manufacturing process (CAD model, Printing, printed coupons) used to produce the Penn State University START Lab flat heat transfer coupons with Hastelloy X material.

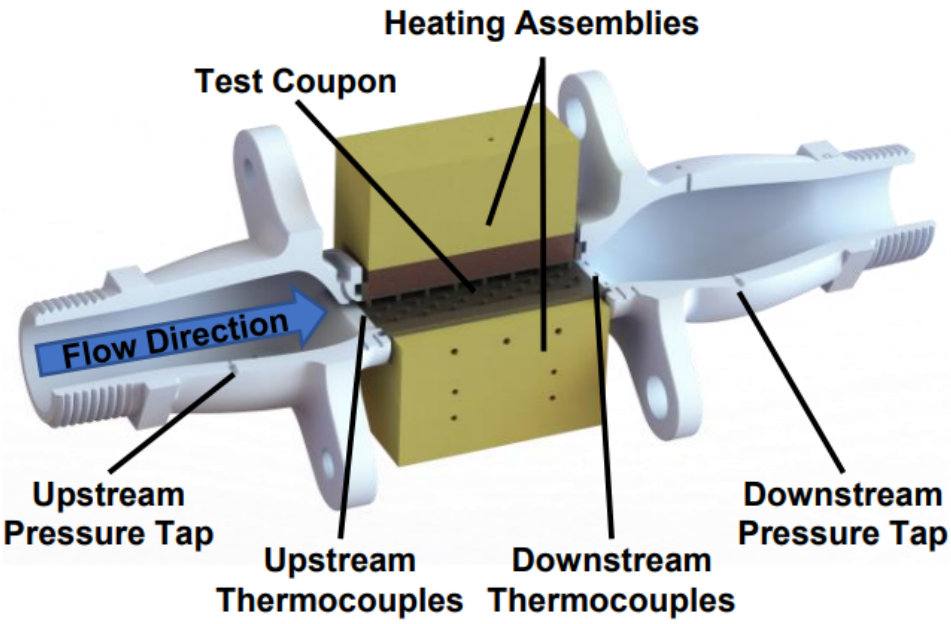

Figure 12. Schematic of the Penn State University START Lab AM Flat Coupon Heat Transfer Test Rig [ref. 1]

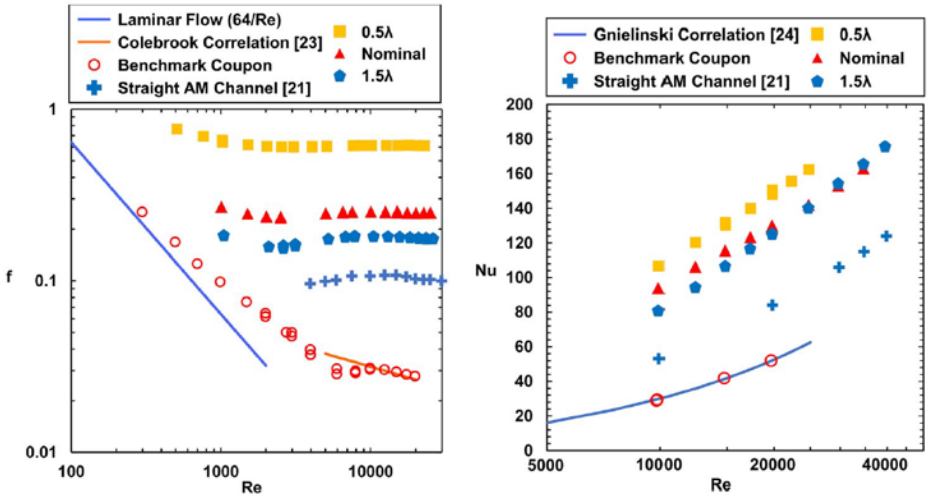

Figure 13. Friction factor (left) and Nusselt number (right) testing results for AM wavy channels produced in AM Hastelloy X coupons. AM results are compared to known correlations for conventional manufactured channels and a straight AM channel (i.e. not wavey) [ref. 1]

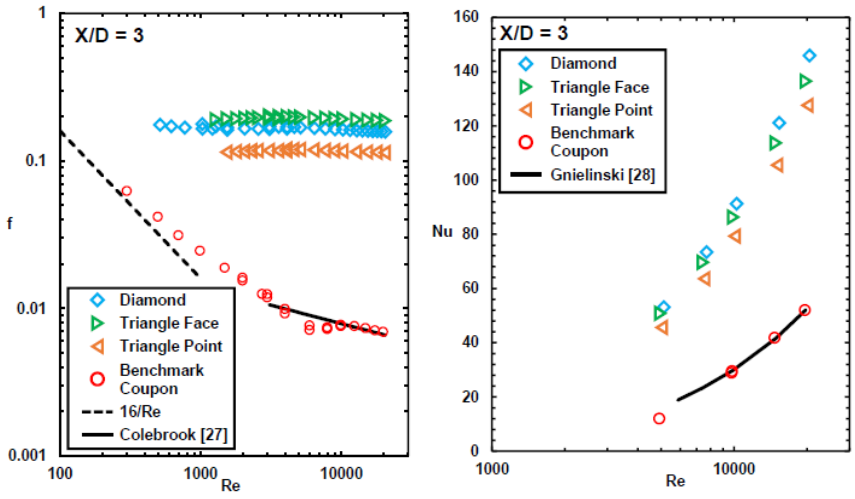

Figure 14 Friction factor (left) and Nusselt number (right) testing results for "Pin Fin" baseline AM HX Flat coupons showing the effects of pin shape and orientation. AM results are compared to known correlations for conventional manufactured channels [ref. 2]

2.4.2 AM Cooled Tip Shoe Component Design

An uncooled tip shoe geometry was digitally modified to incorporate wavy channel and pin fin microchannel cooling architectures into the body of a tip shoe geometry (Figure 15). The thermal properties of the candidate superalloys were incorporated into conjugate heat transfer (CHT) models to assess the effects of the candidate superalloy materials properties on the component predicted metal temperatures during operation. Printability and build orientation of the geometry were also considered to produce a printable design that minimized bulk metal temperatures and thermal gradient.

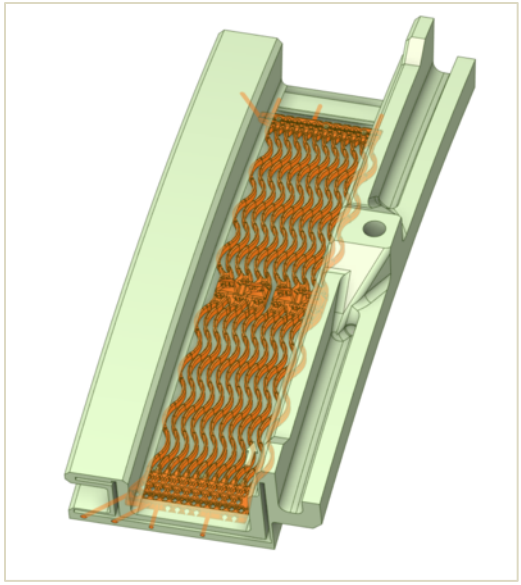

Figure 15 Image of a 3D model of the AM superalloy cooled tip shoe geometry showing the incorporation of AM enabled microchannel cooling architecture.

2.4.3 Predicted Temperature Reduction

Conjugate Heat Transfer (CHT) analysis of the AM superalloy cooled tip shoe geometry was conducted to assess how the allotted amount cooling flow would affect component metal temperatures. When using the same amount of cooling air budget for both the solid and AM cooled geometry, the AM cooled geometry metal temperatures were significantly reduced and areas with high thermal gradients were also reduced (Figure 16). For this original solid tip shoe cooling air budget scenario, the peak metal temperature of the AM cooled tip show flow path centerline metal surface temperature was reduced by greater than 111°C (200F) when compared to the conventional solid tip shoe. Additionally, a trade-off analysis was conducted to assess the effects of reducing allocated cooling flow, and when cooling flow was reduced by approximately 50%, compared to the original design, the AM cooled tip shoe reduced flow design had a flow path centerline metal surface temperature more than 94°C (170°F) cooler than the conventional solid tip shoe design (Figure 17).

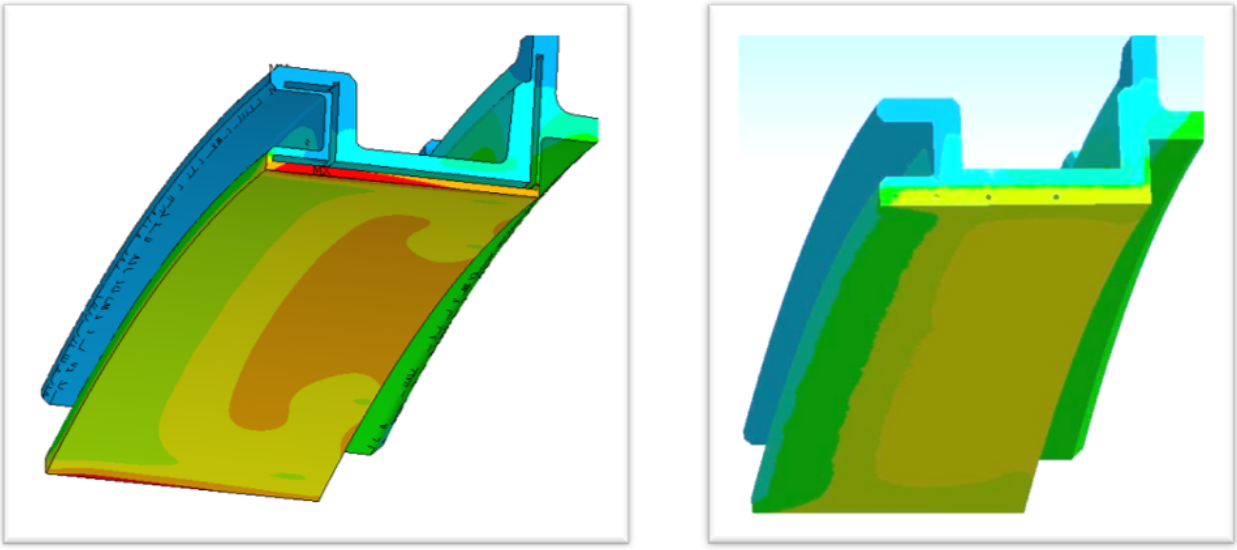

Figure 16. Images of CHT thermal simulation results of a solid tip shoe design (left) and the AM cooled tip shoe design (right) showing a hot side reduction in thermal gradients and metal temperatures for the AM cooled tip shoe design.

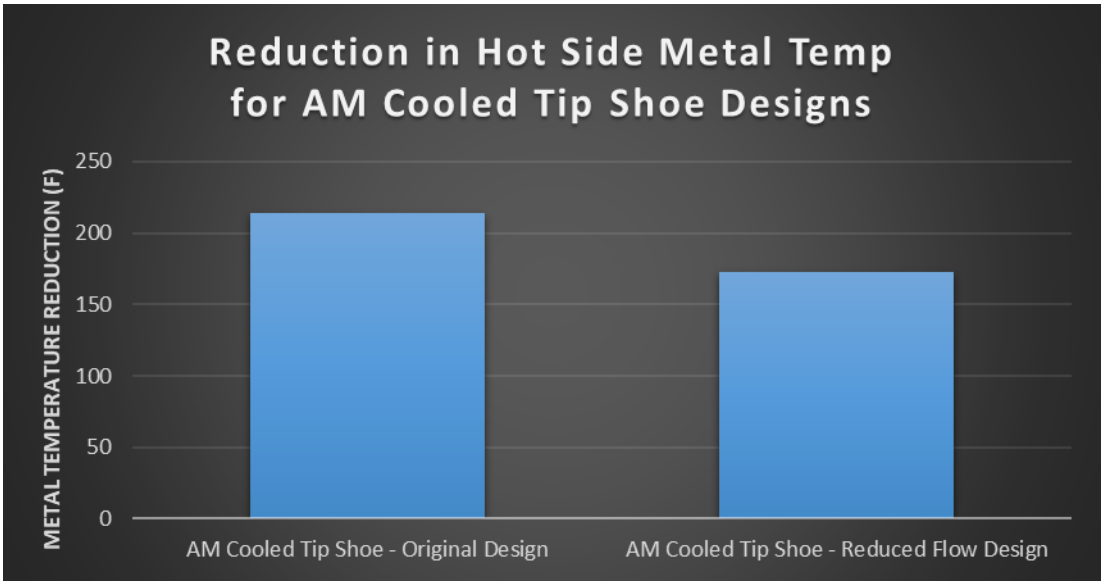

Figure 17. Graph showing the reduction in hot side metal temperature for AM cooled tip shoe designs relative to a solid backside impingement cooled tip shoe design. Temperature reductions were between 119°C (214°F) for the design with the original cooling flow and 96°C (173°F) for the reduced cooling flow design.

2.4.4 Predicted High Temperature Creep Improvements

Mechanical properties curves were fitted to the GP-700 and GP-1100 creep rupture LMP results (see Figure 8) and the increase in temperature capability for the candidate alloys was calculated for stress levels and time scales representative of a turbine tip shoe component operation. The GP-700 and the GP-1100 alloys showed an increased temperature capability of 109°C (197°F) and 133°C (240°F) (Table 3).

The estimated creep life of the AM tip shoe geometry was calculated based on 3D mapped component temperature and stresses derived from computational fluid dynamics (CFD) and finite element analysis (FEA) of three design scenarios: a solid uncooled tip shoe, a cooled tip shoe, and a cooled AM superalloy tip shoe. Incorporating the AM microchannel cooling alone (i.e. no material change) clearly reduced the areas with predicted low creep life and provided a predicted life improvement. However, when incorporating both the AM microchannel cooling and the AM superalloy material, the increase in creep life was significantly improved (Figure 18).

Table 3. Comparison of Increased Temperature Capability of AM Superalloys GP-700 and GP-1100 compared to baseline AM Hastelloy X creep capability at stress and time scales representative of a turbine tip shoe application.

Alloy / Target	Bulk Stress (ksi)	Rupture Hours	Increased Temperature Capability (F)
AM Hastelloy X	10	30,000	n/a
GP-700	10	30,000	197
GP-1100	10	30,000	240
Min. Target	10	30,000	192
Stretch Target	10	30,000	401

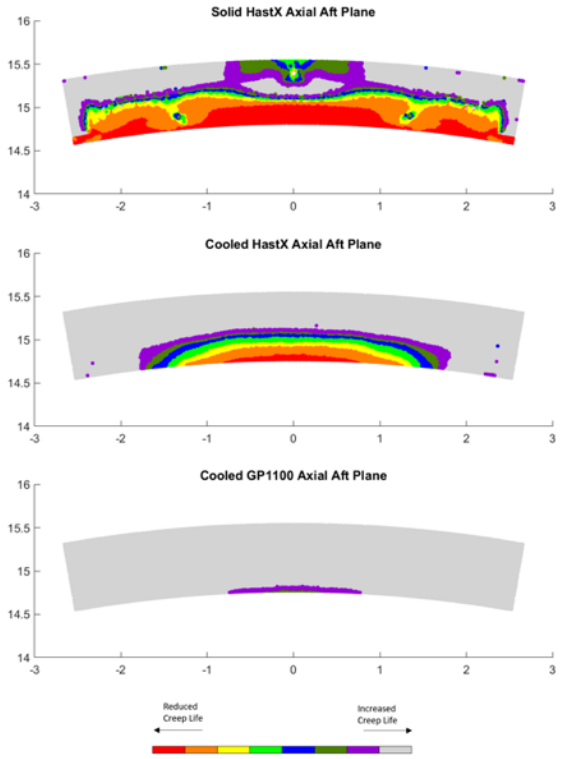

Figure 18. 2D graphical plot of creep life of a solid AM Hastelloy X (Top), Cooled AM Hastelloy X (Middle), and Cooled GP-1100 (bottom) designs showing a significant improvement in life due to incorporation of AM microchannels and the combination of AM microchannels + AM superalloy.

2.4.5 Predicted Engine Performance Effects

There are multiple pathways to increased performance of an industrial gas turbine engine; however, in the specific context of the AM cooled tip shoe component design, two approaches are relevant for this analytical study: (1) a reduction in cooling flow to the tip shoe and (2) supporting a higher turbine rotating inlet temperature (TRIT) increase. While cooling air and TRIT are key elements that are known to contribute to the performance of an engine, once a turbine is actually assembled and operating, there are many other factors that also affect the actual power output including engine-engine build tolerances and ambient operating temperature.

Through a direct part substitution strategy, the reduced cooling flow of a more efficient AM cooled tip shoe provides the opportunity for both a power and efficiency increase for a given TRIT. Alternately, a higher turbine firing temperature would yield significant power increase, however, to realize a higher firing temperature, in addition to the AM tip shoe component, multiple additional turbine components modifications would likely be required.

With this framework in mind, an initial *reduced flow* design scenario was conducted. CFD analysis of the AM cooled tip shoe design showed that when using the same amount of cooling air flow as the incumbent solid tip shoe, the "equivalent flow" AM tip shoe displayed substantial reduction in metal temperature due to the increased cooling efficiencies of the AM enabled internal cooling architecture. Through the combination of improved cooling efficiencies and more capable AM superalloy material enabled a reduced flow AM cooled tip shoe design that still met part durability objectives. A 50% reduction in required cooling air to the tip shoe was achieved which corresponded to a +0.26% power increase.

A second *reduced flow* design study was conducted to evaluate the potential for cooling air savings for a +56°C (+100°F) firing scenario. A higher firing temperature scenario requires additional cooling flow to the tip shoe to maintain durability if the incumbent solid tip shoe technology were used. However, with the AM micro-channel cooling technology, a cooling air reduction of 50% was achieved for the +56°C TRIT scenario, which corresponded to a +0.31% power increase due to air savings relative to the air that would be needed to cool a conventionally manufactured solid tip shoe at this higher firing temperature.

A third pathway was considered to achieve power increase with the AM superalloy tip shoes by means of supporting an overall higher turbine firing temperature. With the combination of greater than 83°C (150 °F) metal temperature reduction with AM cooling (see Figure 17) and greater than 111°C (200F) increase in GP-1100 creep capability (see Table 3), a significant increase in TRIT could readily be sustained by the AM superalloy tip shoes that yielded a predicted power increase well over 1%. However, to implement this higher TRIT approach, clearly additional development work would be required to quantify the effects of the higher TRIT on the surrounding engine components including the blades, nozzle, rings, and disks.

2.5 GP-1100 COMPONENT SCALE-UP BUILDS

GP-1100 was chosen for down-selection for fabrication of the full-scale tip shoe engine components based on the available mechanical property information and GP-1100's favorable high temperature transverse ductility.

With the down-selection of the alloy to GP-1100, subsections of the tip shoe geometry and flow test coupons were printed. Within the initial scale-up prints, the tip shoe components were observed to crack when the HIP operation was performed with the components remaining on the plate. The cracks were consistently located in the radius of the external surface interfacing with the build plate. Cracking still occurred in the base of the tip shoe when performing HIP after part removal from plate as shown in Table 4 which summarizes the empirical investigation into the cracking phenomenon in the GP-1100 tip shoe components.

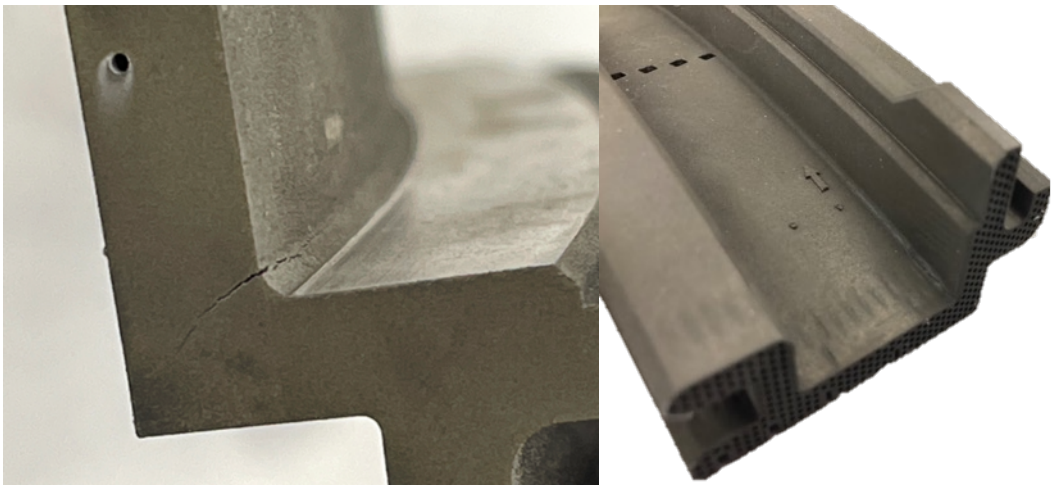

Figure 19: (left) original tip-shoe print + HIP demonstrating cracking. (right) component printed with compliant "honeycomb" structure, EDM'ed off plate, and HIPed still cracking.

Table 4: Crack Mitigation Experiments

Iteration No.	**Process**	**Cracking**
1	Print tip shoe directly to plate, HIP on plate	Yes
2	Print tip shoe directly to plate, remove component via EDM, HIP components without plate	Yes
3	Print tip shoe component onto a compliant structure, remove via EDM, HIP components without plate	Yes – but less severe
4	Print tip shoe component onto compliant thin wall structure, keep components on plate, HIP components with plate	No cracking

To mitigate this observed macro-cracking the solution involved, (1) introducing compliant support structure to minimize residual stress and (2) HIP'ing on the plate to minimize heat-treatment induced distortion (from residual stress relief). The cracking is likely due to the precipitation of gamma-prime during HIP which instantaneously reduces the ductility of the material (ductility dip mechanism). Combined with the distortion driven by high temperature relief of residual stresses results in exceeding the ductility and cracking. Hence, eliminating cracking completely is believed to be achievable by (1) reducing process-induced residual stresses and (2) reducing heat treatment induced distortion. In this case this was achieved by introducing sacrificial compliant material on the bottom of the tip shoe (reduce process induced residual stress accumulation) and HIP'ing while on the plate (constrain the component from deforming and inducing strains).

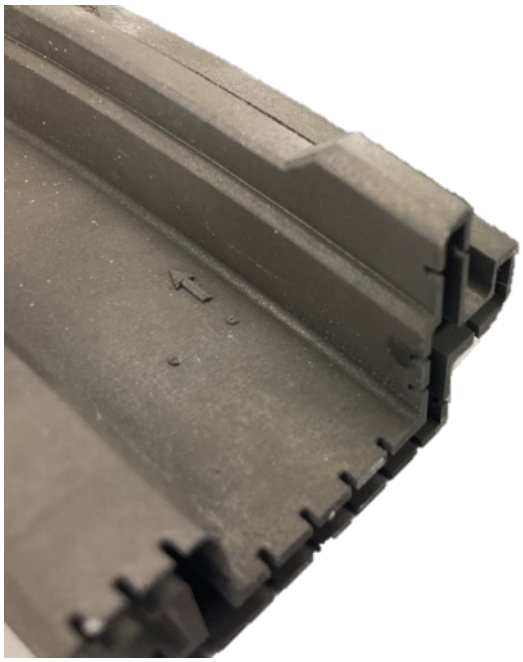

Figure 20: Compliant thin-walled support structure designed to introduce compliance during printing. HIP operation performed with parts on plate to minimize distortion and eliminate cracking.

Following the elimination of cracking during HIP, the components were subsequently aged to allow the material to achieve the optimal microstructure. As expected, with residual stresses relaxed from the HIP, the aging process did not introduce cracking in the concerned region.

After build completion and HIP, parts were imaged using x-ray computed tomography (XCT) to inspect for macro cracking, porosity, and geometrical accuracy of internal features, Blue light scans and XCT were performed on all components after heat treatment as well. Subsequently, the components were machined to the desired tolerances of the alloy and inspected for conformance to those tolerances through coordinate machine measurement (CMM) analysis. A representative fully machined AM superalloy tip shoe is shown in Figure 21.

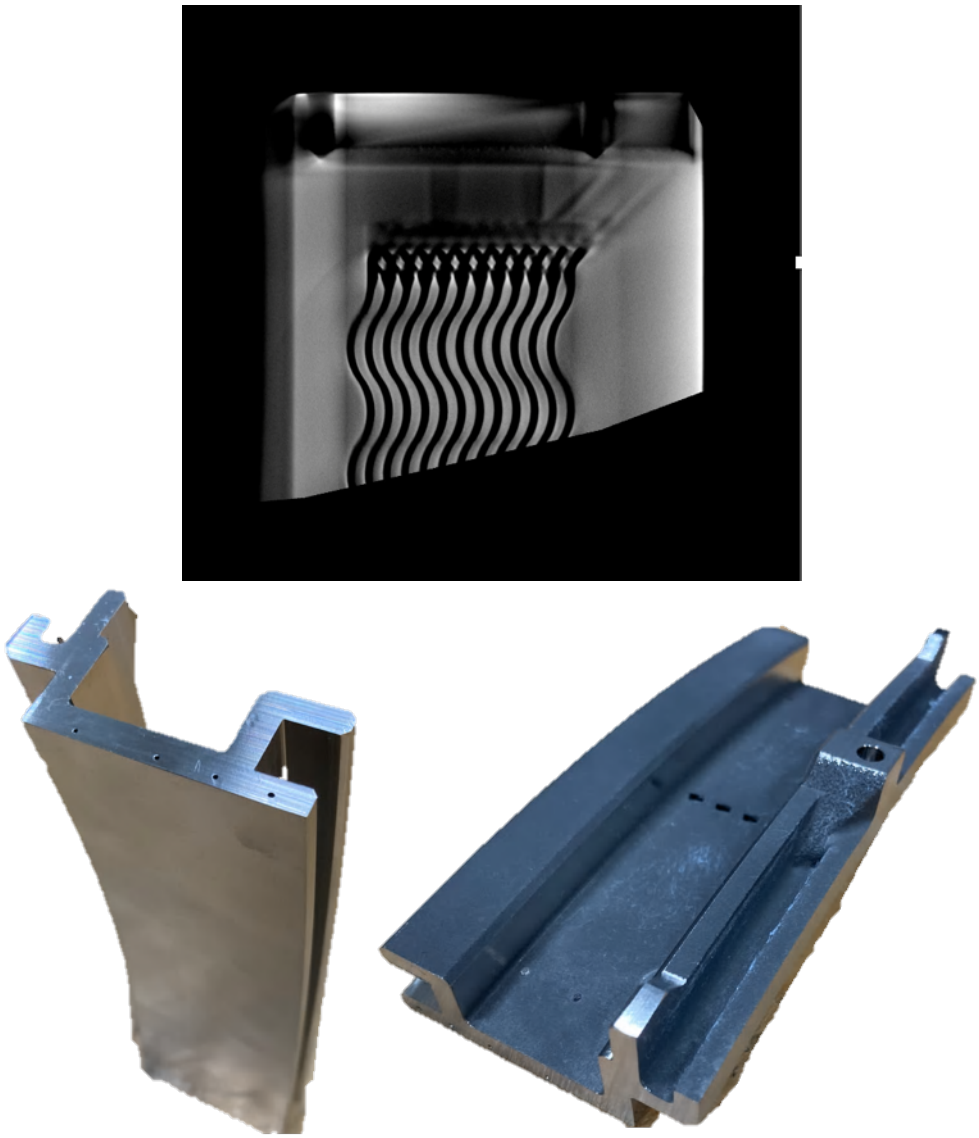

Figure 21: XCT scan of tipshoe component after powder removal (Top); Printed, HIPed, aged, and machined GP-1100 tipshoes (Bottom)

3. IMPACTS

The incumbent manufacturing technology to produce hot-section turbine components is investment casting. Cast superalloy components offer the combination of excellent creep properties and significant geometric complexity needed to ensure the durability and performance of components that operate in the extreme environment of an industrial gas turbine hot flow path. However, the superior performance of these complex castings comes at the cost of long development lead times, high tooling costs, and inflexibility to design changes.

In contrast, AM technology offers the advantages of rapid iterations, elimination of some tooling, and extensive flexibility with incorporating design changes. Yet, despite these advantages, for turbine applications there currently exists significant technology barriers for implementing AM due to limited choices for AM processable high temperature capable alloys. When the legacy Ni-based high gamma prime superalloys are processed using additive manufacturing technologies, the legacy superalloys are prone to severe process induced cracking and reduced high temperature creep properties, and low ductility in the transverse direction.

In this program, significant progress was made with the validation of two next generation high gamma prime superalloys (GammaPrint-700, GammaPrint-1100) that have been specifically designed for AM processability and high temperature capability. The printability of these candidate alloys was demonstrated on prismatic test articles and full-scale proof of concept cooled AM tip shoe components. Additionally, the high temperature creep material properties of the subject AM superalloys showed a significant improvement over baseline AM processable alloys.

Heat transfer and stress analysis of the GP-1100 AM superalloy cooled tip shoe geometry which resulted in a part design with both lower cooling air needs and lower metal temperatures. The resultant tip shoe design is predicted to have a longer creep life and enable operation of the gas turbine with greater efficiency due to the reduction in cooling flow needs. The predicted efficiency gains from the reduced cooling needs translate into a reduced specific fuel consumption and associated reduction in CO2 emissions.

When developing new component designs and implementing product improvements, the hot fired engine performance test is a critical milestone in validating the predicted performance before bringing a turbine engine enhancement to market. By removing the need for investment casting tooling from a project schedule critical path, the time and cost to achieve engine to test can be reduced. Also, the cost of investment cast tooling (typically ranging from $100k to $750k) may be eliminated or deferred. This deferment of locking in the design has the added benefit of allowing for straightforward incorporation of additional design improvements that are revealed during engine testing of the AM produced first articles.

The development of the subject next generation AM superalloys represent a significant step toward industry acceptance of AM processable high temperature material, however, there still remains work to be done to increase the adoption of AM superalloy technology in the gas turbine space. The low transverse ductility dip generally observed in the new class of AM superalloys represents a risk to complex AM part manufacturing yield due to potential of macro-cracking. The low transverse ductility also represents a risk to long term AM part durability while in service due to the fatigue damage mechanism. Additionally, the goal to fully close the creep gap and achieve parity with the incumbent cast superalloys creep properties remains elusive to date. Continued work is recommended to address these limitations with current AM superalloys.

3.1 SUBJECT INVENTIONS

US 11,814,974 B2 Internally Cooled Turbine Tip Shroud Component

Abstract: A tip shroud, comprising a plurality of tip shoes encircling a rotor assembly, in a turbine may deform due to thermal gradients experienced during operation of the turbine. Accordingly, a tip shoe is disclosed that utilizes an internal cooling cavity to supply coolant throughout the interior of the tip shoe, as well as to the slash faces of the tip shoe. In addition, features are described that increase the surface area exposed to the coolant, while remaining suitable for additive manufacturing.

4. CONCLUSIONS

This project was begun on March 22, 2022 and was completed on December 31, 2023. The collaboration partner Solar Turbines is a large business. Through the development efforts of this program ORNL and Solar Turbines integrated AM superalloy material properties data and AM enabled cooling micro-channel geometries into the design of a cooled turbine tip shoe component suitable for operation in a gas turbine engine.

Conclusions and Recommendations:

1. ORNL demonstrated processability of two next generation AM superalloy compositions: GammaPrint®-700 and GammaPrint®-1100 with the test bars and tip shoe components printed on commercially available Laser Powder Bed Fusion (LPBF) systems.
2. Mechanical testing performed by ORNL and Solar Turbines (Thermal physical, Tensile, Creep Rupture, Low Cycle Fatigue) confirmed candidate AM superalloy high temperature creep properties were superior to baseline AM processable alloys and met the minimum project target.
3. The emerging class of next generation AM gamma prime strengthened superalloys display relatively low transverse ductility in the high temperature ductility dip region that pose a risk to full scale component manufacturability and in service part durability. Additional future development is recommended to improve the transverse ductility dip behaviour of the next generation AM superalloy class of alloys.
4. Heat transfer testing conducted at the Pennsylvania State University Steady Thermal Aero Research Turbine (START) Laboratory demonstrated the improved thermal performance of AM micro-channel architectures relative to baseline conventionally manufactured channels.
5. Solar Turbines incorporated the AM superalloy material data and the AM micro-channel architectures into a cooled tip shoe design capable of efficient operation in an industrial gas turbine engine. The AM superalloy design is predicted to have reduced cooling flow needs, lower metal temperatures, and longer creep life compared to the baseline solid tip shoe design.
6. Future experimental validation in the form of hot rig testing or engine testing is needed to validate the actual performance and durability of the subject AM superalloy cooled tip shoe designs.

5. PARTNER BACKGROUND

Solar Turbines Incorporated, a wholly owned subsidiary of Caterpillar since 1981, headquartered in San Diego, California, employs more than 9,000 employees, many of which are located at the headquarters in San Diego, California. Solar Turbines is a leading industrial gas turbine OEM, offering a range of gas turbines and turbomachinery equipment in the 1- 39 MW range for oil & gas exploration and transmission, and for power generation and cogeneration. Solar Turbines' state-of-the-art gas turbines are complemented by a line of compressors that can be matched with Solar Turbines equipment, or that of other OEMs. More than 16,000 Solar units are installed in more than 100 countries accounting for more than 3 billion fleet operating hours.

Solar Turbines has over 50 years of experience with the design, development and commercialization of industrial gas turbines and turbomachinery products. Solar Turbines has a long record of development of gas turbine technologies from internally funded and government programs. An example of a successful government-industry partnership was the DOE-Solar Advanced Turbine Systems (ATS) program, which resulted in the development of the 4.6 MW Mercury^{TM} 50 recuperated gas turbine. Solar Turbines has also been involved in the development of gas turbine products for renewable energy including hydrogen, bio-gas and solar energy.

6. REFERENCES

[1] A. Tadros, G. Ritter, C. Drews, D. Ryan. DOE Technical Report:55232GTH, Additive Manufacturing of Fuel Injectors (2017).

[2] K. Harris and G. Erickson and R. Schwer. Mar-M247 Derivative-CM247LC-DS Alloy CMSX Single Crystal Alloys Properties and Performance in Superalloys 1984, pp 221-230 (1984).

[3] D. Jablonski. Ph.D. Thesis, Fatigue Behavior of Hastelloy-X at Elevated Temperatures in Air, Vacuum, and Oxygen Environments (1978).

APPENDIX A. Technical Papers Associated with CRADA Work

APPENDIX A. TECHNICAL PAPERS ASSOCIATED WITH CRADA WORK

[1] Corbett, T. M., Thole, K. A., and Bollapragada, S. (October 20, 2022). "Amplitude and Wavelength Effects for Wavy Channels." ASME. *J. Turbomach*. March 2023; 145(3): 031011. https://doi.org/10.1115/1.4055612

[2] Corbett, TM, Thole, KA, & Bollapragada, S. "Impacts of Pin Fin Shape and Spacing on Heat Transfer and Pressure Losses." *Proceedings of the ASME Turbo Expo 2022: Turbomachinery Technical Conference and Exposition*. *Volume 6B: Heat Transfer — General Interest/Additive Manufacturing Impacts on Heat Transfer; Internal Air Systems; Internal Cooling*. Rotterdam, Netherlands. June 13–17, 2022. V06BT15A022. ASME. https://doi.org/10.1115/GT2022-82673

[3] Corbett, TM, Thole, KA, Ryan, D, Bollapragada, S, Kirka, M, & Ledford, C. "Impacts of Superalloys on the Surface Quality of Additively Manufactured Channels." *Proceedings of the ASME Turbo Expo 2023: Turbomachinery Technical Conference and Exposition*. *Volume 7B: Heat Transfer — General Interest/Additive Manufacturing Impacts on Heat Transfer; Internal Air Systems; Internal Cooling*. Boston, Massachusetts, USA. June 26–30, 2023. V07BT13A011. ASME. https://doi.org/10.1115/GT2023-102569